Electrical Engineering
https://doi.org/10.1007/s00202-020-01180-7

ORIGINAL PAPER

Optimization of overhead transmission lines insulation and grounding costs with respect to backflashover rate

P. M. De Oliveira-De Jesus[1] · J. C. Amaya[2] · A. L. Acevedo[2] · A. J. Urdaneta U[3]

Received: 3 July 2020 / Accepted: 1 December 2020

Abstract
In this paper, the optimization of transmission insulation and grounding is performed considering two backflashover rate (BFR) evaluation procedures widely applied in the industry. The optimization approach is based on the Lagrange formulation introduced by Hileman in late sixties. This method used the old AIEE procedure to evaluate the BFR of transmission lines. Since then a number of BFR evaluation are available to determine BFR rates outperforming legacy procedures. Recently, the Hileman's optimization method was updated using the EPRI two-point method to evaluate the BFR. However, despite the step-by-step EPRI method being still widely used in industry, stochastic simulation with specialized programs is becoming standard. Thus, in this paper, the insulation and grounding optimization methodology is updated using more adequate and recent BFR evaluation procedures such as the IEEE Std. 1243-97 and the Monte Carlo EMTP-based methods. Technical and economic results were compared with the existing optimization approach based on the EPRI two-point method using the EPRI 345 kV transmission line as test system. Results show that IEEE and EPRI methods yield equivalent results. The stochastic-based method (MC-EMTP) is more optimistic showing total and marginal insulation and grounding costs below the IEEE/EPRI methods.

Keywords Transmission line · Investment costs · Tower grounding · Insulation · Backflashover · Flashover · Reliability · Lightning · Power transmission economics

1 Introduction

Reliability of transmission lines is strongly related to lightning activity. One of the main causes of disruption is the insulation backflashover (BF). Backflashover phenomenon can be mitigated by adding supplemental grounding electrodes, installing line arresters and/or increasing the insulation level [1]. The cost of the insulation equipment and grounding electrodes required to fulfill an accepted/desired reliability level can be sizable in areas with high soil resistivity and/or lightning flash density.

✉ P. M. De Oliveira-De Jesus
pm.deoliveiradejes@uniandes.edu.co

A. J. Urdaneta U
alberto@usb.ve

1 Department of Electrical and Electronic Engineering, School of Engineering, Universidad de los Andes, Bogotá, Colombia

2 Department of Electrical and Electronic Engineering, Universidad de los Andes, Bogotá, Colombia

3 Universidad Simón Bolivar, Caracas, Venezuela

Overestimation in grid infrastructure costing is a fundamental issue for electricity regulatory boards [2]. Nowadays, the seek of economic efficiency is acquiring relevance. According to [3], the mitigation measures are in dire need of engineering challenges and economic improvements since it is not only necessary to increase system reliability but also to reduce the costs of the mitigation measures to the minimum. Optimization is crucial to detect unwarranted expenses in backflashover-related mitigation measures.

In 1967, a method for investment cost optimization of the mitigation measures was proposed by Hileman [4]. This seminal contribution presented the concept of total and incremental cost of the grounding and insulation using Lagrange theory. Figure 1a, b show the original Hileman's total and incremental cost curves for a prescribed backflashover rate range, respectively [4].

The meaning of these curves is the following. For instance, in Fig. 1a, for performance target of 0.004 annual backflashovers per tower, there is a grounding electrode design (with the required impulse grounding resistance to limit the BFR) whose optimal total cost is about $US 1000 and the

Published online: 10 January 2021

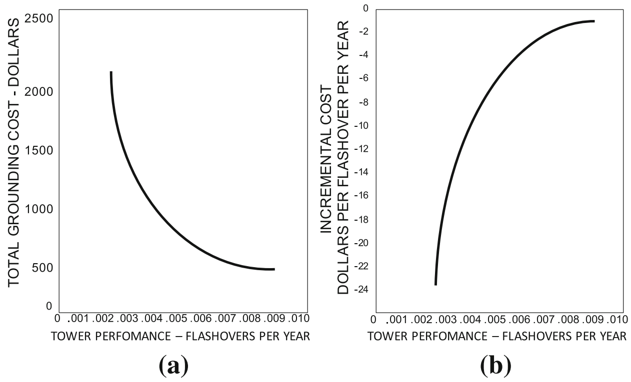

Fig. 1 **a** Total cost, and **b** incremental cost of a transmission line according to Hileman [4]

Table 1 State of the art on BFR optimization

Author, year	Optimization method	BFR method
Hileman, 1967 [4]	NLP	AIEE1950 [5]
De Oliveira, 2002 [7]	MILP	EPRI1975 [8]
Ekonomou, 2006 [9]	NLP	EPRI1982 [12]
Ekonomou, 2009 [10]	NLP	EPRI1982 [12]
Hincapie, 2017 [13]	LP	EPRI1982 [12]
De Oliveira, 2018 [11]	MILP	EPRI1982 [12]
Urdaneta, 2018 [14]	MOLP	EPRI1982 [12]
De Oliveira, 2020 [15]	NLP	EPRI1982 [12]
Amaya, 2020 [17]	NLP	EPRI1982 [12]
This paper	NLP	IEEE1997 [19]
		MC-EMTP [6]

incremental cost is $US -16.0 per flashover per tower. For instance, in a 100 km line with 300 towers if we want to ensure a BFR of 0.4 flashover/100km-yr, the optimal total cost is about $US 300000 and the incremental cost is $US -48000 per flashover/100km-yr.

Notice that the total cost function behaves as a Pareto curve. The trade-off between optimal investment and performance is clear. Achieving high performance indexes (low backflashover rates) will require more expensive mitigation measures. On the other hand, the incremental cost curve depicted in Fig. 1b, can be interpreted as follows: the improvement of 25 % of the BFR (from 0.004 to 0.003 flashovers per tower) will require an additional (incremental) investment -16.0 $US per flashover per tower. This means that if we want to reduce the BFR of 100km line with 300 towers we need an additional investment of $US 16.0 per tower or $US 48000 for the entire line.

Functions shown in Fig. 1 were built using the legacy AIEE [5] method to evaluate the BFR. In the last fifty years, several methods have been proposed to determine the backflashover rates (BFR) in flashovers per 100km per year including many new features that were not known in the late sixties such as grounding impulse representations, statistical lightning parameters and advanced simulation programs such as the Electromagnetic Transients Program (EMTP) [6].

Economic optimization to reduce backflashover rates has been clearly overlooked in the literature. In practice, the design processes to address the consequences of the backflashover phenomenon have been based primarily on simulation rather than optimization. However, besides the legacy Hileman's approach introduced in 1967, we can find a number of recent approaches that address the optimization problem for a prescribed BFR range.

Table 1 lists existing papers concerning grounding and insulation optimization with respect to the BFR from economic viewpoint. The list is sorted by year, optimization technique and flashover rate evaluation method used. The selection of supplemental grounding electrodes to fulfill an accepted/desired BFR is presented in [7] using mixed integer linear problem (MILP) and the general procedure to compute the BFR of transmission lines introduced by the Electric Power Research Institute (EPRI) in 1975 [8]. Ekonomou presented two practical studies where grounding and insulation costs were optimized using nonlinear programming (NLP) [9,10]. The MILP formulation was extended in [11] in order to include the insulation costs in the objective function of the optimization problem applying the second version of the EPRI [12] step-by-step procedures two-point method. In [13], the optimization process is carried out using the simplex Nelder–Mead optimization method. In [14], insulation and grounding costs are jointly analyzed as a multiple objective linear optimization problem (MOLP).

Recently, the legacy Hileman's optimization method was updated by [15] using the EPRI two-point method to assess the back flashover rate [12]. The updated nonlinear programming method (NLP) includes a specific representation of impulse grounding resistances [16]. The optimization method presented in [15] was also applied by [17] to analyze HVDC systems using the EPRI BFR calculation approach.

However, despite the EPRI two-point method still widely used by planners to determine the transmission backflashover rates due to backflashover [12], authors [18] claim that classic step-by-step probabilistic methods have been upgraded by stochastic-based methods such as the one standardized by the IEEE Std. 1243 [19] (IEEE Flash program) and several approaches based on Monte Carlo EMTP simulation [6]. Thus, the optimization methodology should be tested using more adequate and recent BFR evaluation procedures.

To fulfill the research gap, this paper applies the optimization approach introduced by Hileman [4] and updated by [15] to determine optimal investment cost curves (total and incremental) for mitigation measures (grounding and insulation) considering two standard BFR evaluation pro-

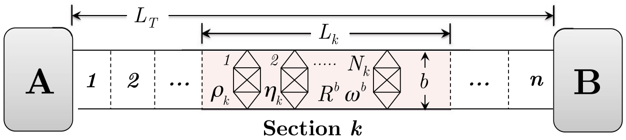

Fig. 2 Transmission line scheme [15]

cedures: IEEE Std. 1243-1997 [19] (Flash Program), and the Monte Carlo-EMTP method [6]. The EPRI two-point method [12,15] is used as reference case. By updating the Hileman's optimization approach, we can compare different existing BFR evaluation methods from the economic perspective, i.e., the optimal investment cost of the mitigation measures required to achieve an accepted/desired reliability level.

The authors are aware that there are other BFR procedures such as the CIGRE Brochure 063-1991 [20] and a myriad of Monte Carlo EMTP/ATP/PSCAD-based applications [6,21,22] that deserve to be benchmarked. However, due to space constraints, in this paper we only consider two methods: IEEE Std. 1243-1997 and MC-EMTP. We encourage further research and development of the methodology considering all existing methods to evaluate the BFR of transmission lines.

The paper is organized in the following manner. Section 2 presents a brief review of the BFR evaluation methods used. Section 3 presents the optimization model used. Results obtained from a case study are discussed in Sect. 4. Conclusions are drawn in Sect. 5.

2 Backflashover rate evaluation methods

The backflashover rate (BFR) of a transmission line, hereafter denoted as T, accounts the expected number of flashes per 100 km per year due to backflashover phenomenon [19]. Before describing how the T parameter is calculated using different methods, some previous definitions are required.

Figure 2 depicts a generic transmission line linking a substation A with a substation B. The total length is given by L_T. The line can be single or multi-circuit. The line is divided in n sections grouping a number of adjacent towers considering similar resistivity and flash density conditions. Table 2 shows the basic dataset required to elaborate the optimization model. Besides resistivity and flash density data, transmission line and tower geometry should be defined at each section k. Buried parts of transmission towers have a base impulse footing resistance also dependent on local earth resistivity.

Since 1950 several BFR evaluation methods have been developed by a number of researchers and institutions using the dataset defined in Table 2. A detailed description of the history of BFR methods can be found in [23,24].

Table 2 Technical dataset

Variable	Description (unit)
N_k	Number of towers at each section
L_k	Section length, km.
ρ_k	Soil resistivity at section k, Ω-m.
η_k	Density in section k, flashes per km^2-yr.
R^b	Base tower impulse resistance, Ω.
w^b	Base insulation (string length), cm
w^{mx}	Maximum string length, cm.
b_k	Distance between the shielding wires, m.
H_k	Tower height at section k, m.

In this paper, optimization method developed by [15] is carried out considering the EPRI method as reference and two methods (IEEE and MC-EMTP) reported in the literature to evaluate back flashover rates:

1. $h = 1$: EPRI method (Reference) [12,15],
2. $h = 2$: IEEE Std. 1243-1997 method [19],
3. $h = 3$: Monte Carlo-EMTP method [6,21].

For each method h, the global backflashover rate T_h of the transmission line is computed using the following composite formula [19]:

$$T_h = \sum_{k=1}^{n} T_{k,h} \frac{L_k}{L_T} \tag{1}$$

where $T_{k,h}$ is the specific BFR at each section k for method h in flashovers/100km-yr. The BFR at each section k ($T_{k,h}$) is defined by Eq. 2 as the product of two components: the frequency of flashes per 100km-yr (μ_k) and the cumulative probability of such flashes terminate in the tower shielding structure producing a backflashover ($P_{ck,h}$):

$$T_{k,h} = \kappa \mu_k P_{ck,h}[I_k > I_{ck,h}(w_{k,h}, R_{k,h})] \tag{2}$$

where κ is a constant equal to 0.6 [12,19]. In this paper, for comparison purposes, parameter κ and the annual frequency (μ_k) are the same in all BFR methods. On the other hand, the cumulative probability ($P_{ck,h}$) will adopt a different value in each BFR method h. In the following, we briefly describe the features of cumulative probability of the backflashover and direct strokes frequency assessment for the all methods under study.

2.1 Cumulative probability of the backflashover

The cumulative probability of a lightning current amplitude is defined by the frequency that the stroke current (I_k, in kA) exceeds the critical current ($I_{ck,h}$, in kA) required to provoke backflashover at section k. The insulation breakdown is modeled through the critical flashover overvoltage (CFO) in kV [12]. The CFO is the crest value of the impulse wave for which the probability of flashover occurrence is 50 % [19].

$$CFO_{k,h} = 0.4 w_{k,h} + 0.71 w_{k,h} t^{-0.75} \tag{3}$$

where $w_{k,h} \in \boldsymbol{w_h}$ is the optimal insulation length in cm and t is the time in microseconds. The optimal insulation length has upper and lower bounds: $w^b \leq w_{k,h} \leq w^{mx}$, with w^b and w^{mx} defined in Table 2.

The backflashover occurs at section k when at given time t, the overvoltage produced by the lightning strike $\Delta V_{k,h}(t)$ exceeds the CFO of the line at section k:

$$\Delta V_{k,h}(t) = V_{Tk,h}(t) - V_{pk}(t) > CFO_{k,h} \tag{4}$$

where the term $\Delta V_{k,h}(t)$ is the insulator stressing voltage considering the effect of the operational voltage, $V_{Tk,h}(t)$ is the stressing voltage corresponding to the difference between the ground potential rise and the coupled voltage from the traveling waves on the shield-wires to the phase conductor, and $V_{pk}(t)$ is the operating voltage at phase k.

When a flash terminates in the line, two main voltage components are developed. First, we have a potential rise on the tower cross-arm due to traveling waves going down through the tower and reflecting into the grounding resistance. On the other hand, the traveling waves through the shielding wires will give rise to voltage directly coupled to the phase conductors. The difference of these two components is the insulator stressing voltage ($V_{Tk,h}(t)$). As the line is energized, the operating voltage ($V_{pk}(t)$) will increase or decrease the stressing voltage depending on the moment of the cycle the lightning strike occurs.

The tower cross-arm voltage depends on the lightning strike current, the couplings between all conductors, the tower self-inductance and the optimal footing resistance including supplemental grounding electrodes $R_{k,h} \in \mathbf{R_h}$. The optimal grounding resistance has an upper bound: $R_{k,h} \leq R^b$, with R^b defined in Table 2.

The backflashover depends on the specification of both the optimal impulse resistance of the tower and the optimal insulation level of the tower at given section. The term "optimal" means that the specified value (by design) of grounding resistances (the number of counterpoises) and insulation lengths (the number of insulators) are obtained as a result of an optimization procedure that aims to minimize grounding and tower structure costs for a given reliability level specified by the planning engineering board.

Table 3 Statistical parameters of first negative and positive return-strokes current [21,22]

Parameter	Median value	Standart deviation
I_p	35 kA	1.21
t_f	22 μs	1.23
t_T	230 μs	1.33

The cumulative probability can be obtained by different ways depending on the BFR method used:

$$\text{EPRI \& IEEE: } P_{ck,1} = P_{ck,2} = \left(1 + \left(\frac{I_{ck,h}}{31}\right)^{2.6}\right)^{-1} \tag{5}$$

$$\text{MC-EMTP: } P_{ck,3} = {}^{M_{flash}}/_{M} \tag{6}$$

The EPRI and IEEE methods determine the cumulative probability using the Anderson Equation 5. The calculation of the cumulative probabilities $P_{ck,1}$ and $P_{ck,2}$ for the EPRI and IEEE method is determined using a step-by-step procedures whose details can be consulted in [12] and [19], respectively. The Monte Carlo-based method [6,21] determines the cumulative probability ($P_{ck,3}$) assessing the statistical behavior of the transmission line. The Monte Carlo procedure generates lightning strikes, assumed to terminate within a 1-km-wide swath centered on the overhead transmission line [22]. The strokes are simulated by the ATP/EMTP program with a detailed model for the line tower [6,21]. Statistical modeling of line insulation breakdown, yields M_{flash} total flashovers out of M strokes. Statistical representation of lightning stroke parameters (peak current I_p, front time t_F and tail time t_T) has been assumed to follow a log-normal distribution, with probability density function [21,22]:

$$p(x) = \frac{1}{\sqrt{2 \cdot \pi} x \sigma_{\ln x}} \cdot \exp\left[-\frac{1}{2}\left(\frac{\ln x - \ln x_m}{\sigma_{\ln x}}\right)^2\right] \tag{7}$$

where $\sigma_{\ln x}$ is the standard deviation of $\ln x$ and x_m is the median value of x. Values used in this paper are taken from [21,22] and listed in Table 3.

2.2 Expected annual direct stoke frequency

Expected annual direct stoke frequency (μ_k) depends on two parameters: the annual flash density (η_k) obtained from flash detectors and the tower geometry using a shadow length (S_k):

$$\mu_k = 0.1 \eta_k S_k \tag{8}$$

The EPRI method uses a shadow length ($S_k = 4H_k^{1.09} + b_k$) narrower than the one used by the IEEE method ($S_k = 28H_k^{0.6} + b_k$). The shadow length of each section of the line (S_k) depends on the tower height (H_k) and the distance between the shielding wires (b_k) previously defined in Table 2. In this paper, all BFR evaluation methods (EPRI, IEEE and MC-EMTP) use the same expression (Eq. 8) to determine μ_k.

3 The optimization model

Hileman [4] proposed in 1967 a nonlinear optimization problem (NLP) where the investment cost of mitigation measures (grounding and insulation), i.e., the tower grounding and insulation costs, is constrained to a lightning performance function. The backflashover rate (BFR) was determined using the old AIEE method [5]. The general problem formulation can be written as follows: determine the optimal grounding and insulation design scheme such that

$$\begin{aligned}&\text{minimize Grounding}(\boldsymbol{R}) \quad \& \quad \text{Insulation}(\boldsymbol{w})\text{Cost}\\&\text{subject to:}\\&\text{Estimated BFR function} \quad (\boldsymbol{R}, \boldsymbol{w}) = \text{Target BFR}\end{aligned}$$

The cost of grounding supplemental electrodes is obtained from power frequency grounding resistance using Sunde's equations [25]. The cost of insulation is obtained from [1]. The estimated BFR function is parameterized from the EPRI step-by-step procedure [12].

In this paper, we applied the modified Hileman's optimization model [15] using two different and more recent procedures to evaluate the BFR of the transmission line: IEEE Std. 1247-1997 [19] and the Monte Carlo-EMTP [6,21]. Results obtained are compared with the ones obtained using the EPRI two-point method in [15].

3.1 Estimated BFR functions

According to Hileman [4], solving the optimization problem requires a nonlinear, continuous and differentiable function that relates the BFR with the design variables at tower in all sections of the line: insulation and grounding resistances. Thus, specific functions for BFR, grounding and insulation cost should be developed for each BFR evaluation method. According to Eq. 2, at each section k, the BFR depends on two main design parameters: the impulse resistance of the tower with supplemental grounding electrodes ($R_{k,h} \in \mathbf{R_h}$) and the phase insulation level (string length) ($w_{k,h} \in \mathbf{w_h}$, cm). The relationship between the parameterized backflashover rate ($\widehat{T}_{k,h} \in \mathbf{T_h}$) and the unknown design variables ($R_{k,h}, w_{k,h}$) can be estimated using ordinary least squares method from exact simulation solutions T_h of a given BFR evaluation method $h = \{1, 2, 3\}$. The estimated BFR function for each method h is given by the following equation:

Table 4 Economic dataset

Variable	Description (unit)
σ	Incremental insulation cost, US\$/m
β	Grounding cost factor, US\$
γ	Grounding cost factors, unitless

$$\widehat{T}_{k,h} = f(\alpha_{ij,h}; w_{k,h}, R_{k,h}) = \sum_{i=1}^{m}\sum_{j=1}^{m} \alpha_{ij,h}\eta_k w_{k,h}^i R_{k,h}^j \quad (9)$$

where the flash density $0 \le \eta_k \le \eta^{mx}$ is a known value that varies along the line. Insulation and impulse resistances are limited: $w^b \le w_k \le w^{mx}$, $R_k^{min} \le R_{k,h} \le R^b$. R_k^{min} and R^b are the minimum and maximum grounding resistance value. Parameter m is the fitting polynomial order. $\alpha_{ij,h} \in \boldsymbol{\alpha_h}, \forall i, j = 1, ..., m$ are the regressors of each BFR method h. Estimation of $\widehat{T}_{k,h}$ is carried out using the following BFR calculation procedures: $h = 1$, the EPRI method (base case); $h = 2$, the IEEE Std. 1243-1997 method (IEEE Flash program), and $h = 3$, the Monte Carlo EMTP method. A detailed description about the parameterization process is provided in [15].

3.2 Estimated cost functions

For BFR evaluation method h, the insulation and grounding costs are determined as a function of the state variables: insulation lengths and impulse resistances. For the sake of simplicity, the inclusion of line arresters is not considered and matter of future research. Basic economic data required by the optimization process are listed in Table 4. The insulation length $w_{k,h}$ is defined by the number of insulators of the string. On the other hand, the impulse resistance $R_{k,h}$ is defined by electrode geometry. According to [15], we can define the insulation $C_{Ik,h}$ and grounding costs $C_{Gk,h}$ at each section k as follows:

$$C_{Ik,h} = N_k\sigma(w_{k,h} - w_k^b) \quad (10)$$

$$C_{Gk,h} = N_k\beta\left[\frac{\rho_k}{R_{0k,k}}\right]^{\gamma} \quad (11)$$

$$R_{0k,h} = \sqrt{\frac{\rho_k G_0 R_{k,h}}{\rho_k G_0 - 62\pi \sqrt[5/13]{\frac{\widehat{T}_{k,h}}{0.6\mu_k}} R_{k,h}^2}} \quad (12)$$

where N_k is the number of towers at section k, G_0 is the ionization field gradient in kV/m (500 kV/m) and, ρ_k is the earth resistivity in Ω-m. The insulation cost of a given section depends on σ, defined in [15] as the incremental cost of insulation in (US\$/m). Changes on insulation lengths produce additional costs due to tower structure resize. The installation cost of supplemental grounding electrodes at a given section k is expressed as a function of the power frequency grounding resistance ($R_{0k,h}$) where fitting factors γ and β are acquired from the parameterization of Sunde's equations [25]. These power frequency resistances can be easily measured using the IEEE Std. 81-2012 [26]. The relationship between the power frequency grounding resistance $R_{0k,h}$ and the grounding impulse resistance $R_{k,h}$ is nonlinear as seen in Eq. 11. The optimization problem determines the impulse resistance $R_{k,h}$ as state variable according to the minimal cost of $R_{0k,h}$.

Several approaches have been introduced to link steady-state and dynamic grounding resistances. For the sake of simplicity, Eq. 11 is derived from the well-known formula for concentrated supplemental electrodes (with counterpoise lengths lower than 30 m) [16,20].

$$R_{k,h} = \frac{R_{0k,h}}{\sqrt{1 + I_{ck,h} / \frac{\rho_k G_0}{2\pi (R0k,h)^2}}} \tag{13}$$

where $I_{ck,h}$ is the critical current to provoke backflashover in kA. The critical current also can be obtained from Eq. 5 as a function of the estimated BFR ($\widehat{T}_{k,h}$) given in Eq. 9 and the design variables ($R_{k,h}$, $w_{k,h}$):

$$I_{ck,h} = 31 \sqrt[5/13]{\frac{\widehat{T}_{k,h}}{0.6\mu_k}} \tag{14}$$

Further details about the cost functions of supplemental grounding electrodes are provided in [15].

3.3 The optimization model

The input parameters of the optimization problem are the transmission line dataset defined in Table 2 (environmental, physical structure and geometry data) and the fitting coefficients obtained from the parameterization process presented in Sect. 3.2 for each BRF evaluation methodology. The fitting parameters are described as $\boldsymbol{\alpha_h}$ for each BFR procedure $h = \{1, 2, 3\}$. Thus, the optimization problem aims to find for all sections $k = 1, \ldots, n$, impulse resistances $\mathbf{R_h} = \{R_{1,h}, \ldots, R_{k,h}, \ldots, R_{n,h}\}$ and insulation lengths $\mathbf{w_h} = \{w_{1,h}, \ldots, w_{k,h}, \ldots, w_{n,h}\}$ for minimal investment cost ($C_{T,h}$) in grounding ($C_{G,h}$) and insulation ($C_{I,h}$) subject to an accepted/desired overall BFR T^* [15]

$$\min_{\mathbf{w_h},\mathbf{R_h}} C_{T,h} = \sum_{k=1}^{n} N_k \sigma_k (w_{k,h} - w^b) + \sum_{k=1}^{n} N_k \beta \left[\frac{\rho_k}{R_{0k,h}}\right]^{\gamma} \tag{15}$$

subject to:

$$\widehat{T}_h = \sum_{k=1}^{n} \widehat{T}_{k,h} \frac{L_k}{L_T} = T^* \tag{16}$$

$$\widehat{T}_{k,h} = \sum_{i=1}^{m} \sum_{j=1}^{m} \alpha_{ij,h} \eta_k w_{k,h}^{i} R_{k,h}^{j} \; \forall k = 1, \ldots, n \tag{17}$$

$$R_{0k,h} = \sqrt{\frac{\rho_k G_0 R_{k,h}}{\rho_k G_0 - 2\pi I_{ck,h} R_{k,h}^2}} \quad \forall k = 1, \ldots, n$$

$$I_{ck,h} = 31 \sqrt[5/13]{\frac{\widehat{T}_{k,h}}{0.6\mu_k}} \quad \forall k = 1, \ldots, n$$

$$w^b \le w_{k,h} \le w^{mx}, 0 < R_{k,h} \le R^b \quad \forall k = 1, \ldots, n \tag{18}$$

where $C_{T,h}$ is the total cost per method h defined as the sum of grounding costs (Eq. 10) and insulation costs (Eq. 11). Besides the state variables ($R_{k,h} \in \boldsymbol{R_h}$, $w_{k,h} \in \boldsymbol{w_h}$), system frequency grounding resistances $R_{0k,h} \in \boldsymbol{R_{0,h}}$ and BFR $\widehat{T}_{k,h} \in \boldsymbol{T_h}$ per section are relevant output variables.

The overall backflashover rate $\widehat{T}$ of the transmission line in Eq. 16 is computed according to the composite formula provided in 1. The BFR at section k ($\widehat{T}_{k,h}$) in Eq. 17 is the parameterized BFR function defined in Eq. 9 for all BFR evaluation methods defined in Sect. 2. The model is also constrained to Eqs. 13 and 14. State variables $w_{k,h}$ and $R_{k,h}$ are constrained to lower and upper bounds in Eq. 18.

The optimization model stated in 15-18 is nonlinear suitable to be solved with the Matlab's *fmincon* tool (Newton and interior-point method). The λ_h of the system (Lagrangian multiplier associated with Eq. 16) corresponds to the marginal/incremental cost of the BFR in US\$/flashovers /100km-yr for a given BFR evaluation procedure and reliability level target T^*.

In Fig. 3, a flowchart is presented with the overall optimization procedure required to get the total and incremental cost curves as a function of a desired range of backflashover rates $T^* \in [T^{min}, T^{max}]$.

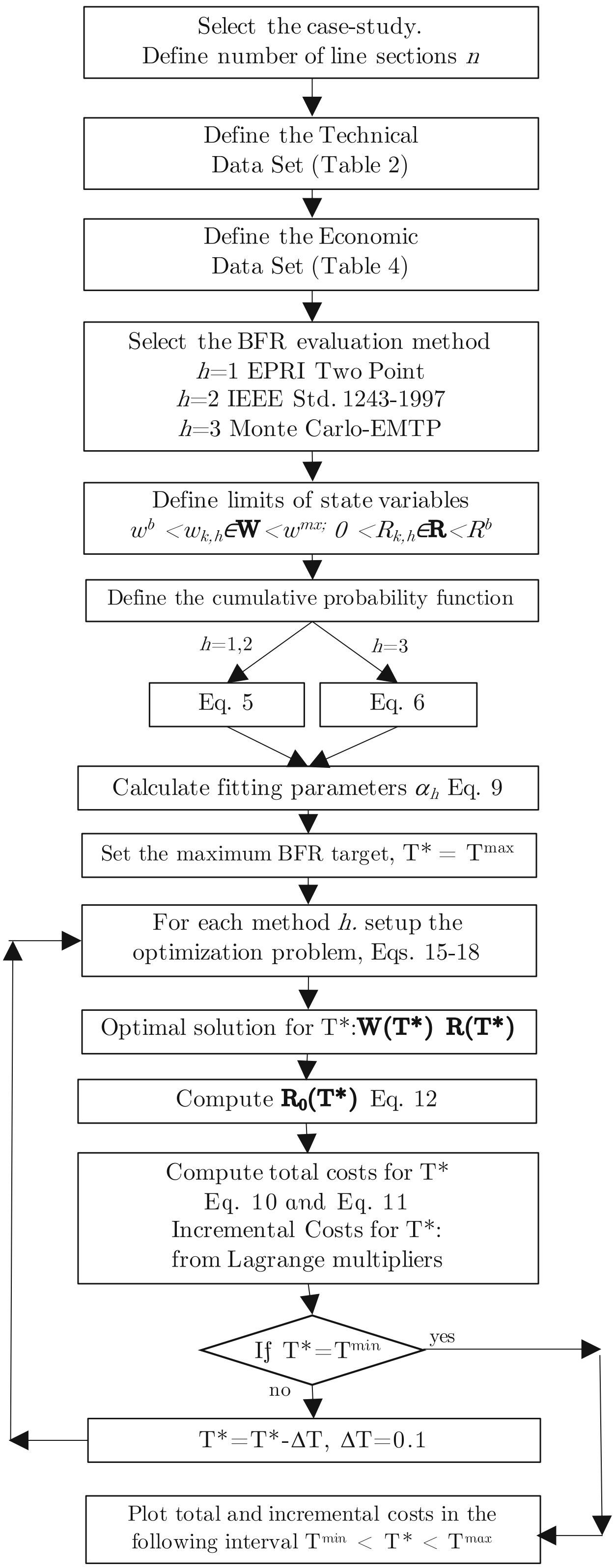

Fig. 3 Optimization procedure flowchart

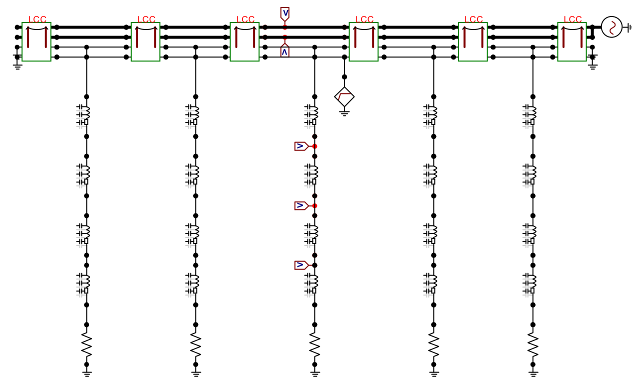

Fig. 4 ATP-EMTP scheme

3.4 Limitations

This paper does not consider frequency dependence of soil electrical parameters in the transient behavior of tower-footing grounding systems. Only concentrated supplemental electrodes are considered. Counterpoise lengths are limited to 30m. Further research is needed to incorporate frequency dependence in the design process.

4 Results and discussion

The optimization model stated in Sect. 3 was applied using two BFR formulations (IEEE and MC-EMTP) and results compared with EPRI case [15]. All cases use the same technical and economic data [15]. The two-circuit 345kV transmission line defined in [12] (Chapter 12) was used as test system. The length of the line is 100km and divided in $n = 12$ sections with 25 towers each. The transmission line dataset (environmental, physical structure and geometry data) is included in Table 5. We assume that the transmission line is perfectly shielded. The interested reader can replicate the results shown in this section by running the ATP and MATLAB scripts included in the following repository: https://github.com/pmdeoliveiradejesus/BackFlashoverOptimization (ELEN folder). Basic circuit used in the ATP-EMTP platform is shown in Fig. 4.

4.1 BFR evaluation for one single line section: *k* = 7

Before to determine the parameterization of the BFR functions and performing the optimization tasks, the BFR is calculated using the EPRI, IEEE and MC-EMTP methods for comparison purposes. Considering that in line section 7 the design parameters are $R_{7,h}$ = 20 ohms, $w_{7,h}$ = 263 cm, Table 6 presents the resulting cumulative probability $P_{c7,h}$, the expected annual direct strokes frequency $\mu_{7,h}$, in

Table 5 Optimization problem dataset

Param.	1	2	3	4	5	6	7	8	9	10	11	12
N_k	25	25	25	25	25	25	25	25	25	25	25	25
L_k (km)	8.3	8.3	8.3	8.3	8.3	8.3	8.3	8.3	8.3	8.3	8.3	8.3
ρ_k (Ω-m)	850	750	1250	1150	975	1125	1500	2400	4000	4200	2000	1800
η_k	4.6	4.6	4.6	4.6	3.6	3.6	3.6	3.6	2.6	2.6	2.6	2.6
R^b (Ω)	500	500	500	500	500	500	500	500	500	500	500	500
w^b (cm)	263	263	263	263	263	263	263	263	263	263	263	263
w^{mx} (cm)	445	445	445	445	445	445	445	445	445	445	445	445
b_k (m)	11	11	11	11	11	11	11	11	11	11	11	11
H_k (m)	39	39	39	39	39	39	39	39	39	39	39	39

Table 6 R results with $R_7 = 20$ ohms and $w_7 = 2.63$ m

Method	$\mu_{7,h}$	$Pc_{7,h}$	$T_{7,h}$
$h = 1$.- EPRI[12]	94.76	0.0242	1.3863
$h = 2$.- IEEE[19]	94.76	0.0300	1.7171
$h = 3$.- MC-EMTP [6]	94.76	0.0216	1.2313

flashes/100km-yr and the backflashover rate calculation $T_{7,h}$ (Eq. 2) for all BFR evaluation methods described in Sect. 2.

In order to compare the BFR calculation methods on the same basis, expected annual direct stoke frequency (μ_7) is set in all cases as: $\mu_7 = 0.1\eta_7(28H_7^{0.6} + b_7) = 0.1 \times 3.6 \times (28 \times 39^{0.6} + 11) = 94.76$ strokes per 100 km. Cumulative probabilities are calculated assuming $R_7 = 20$ ohms and $w_7 = 263$ cm. The EPRI method was scripted in Matlab. The IEEE method was applied using the Flash program [19]. The Monte Carlo approach was run using a Matlab interface with the ATP/EMTP program [6]. The iterative process stops when the change in the probability function is lesser than 10^{-5}. To achieve convergence, 11345 iterations were necessary. The cumulative probabilities obtained by the MC-EMTP and the IEEE methods are lower and higher than the EPRI solution as reported in the step 34 of the two-point method [12] ($Pc_{7,1} = 0.025$), respectively. The MC-EMTP method seems to be optimistic with the lowest BFR, and the IEEE method seems to be pessimistic with the highest BFR. The application of the optimization problem in all methods and over a range of accepted/desired backflashover rates will allows us to compare all procedures under a broader extent.

4.2 Defining the estimated BFR functions

The parameterization of the BFR for each evaluation method was carried out via ordinary least squares setting a polynomial of order of $m = 6$.

$$\widehat{T}_{k,h} = \sum_{i=1}^{6}\sum_{j=1}^{6} \alpha_{ij,h}\eta_k w_{k,h}^i R_{k,h}^j$$

$$0 \le \eta_k \le 4.6 \text{ flashes/km}^2\text{-yr}$$

$$200 \text{ cm} \le w_{k,h} \le 445 \text{ cm}, 0\Omega < R_{k,h} \le 50\Omega \tag{19}$$

Regression solution is given by $\boldsymbol{\alpha_h} = (\mathbf{X}'\mathbf{X})^{-1}\mathbf{X}'\mathbf{T_h}$ where each dependent variable of $\mathbf{T_h}$ is obtained from running a simulation program and $\mathbf{X}$ is the set of independent variables η_k, $w_{k,h}$ and $R_{k,h}$. For example, for the base case EPRI ($h = 1$) at section k=7, the simulated BFR result $T_{7,1}(\eta_7 = 3.6$#/100km-yr, $w_{7,1} = 263$cm, $R_{7,1} = 20\Omega)$ yields 1.3863 flashovers/100km-yr shown in Table 6, and the estimated one using the parameterized function (Eq. 19) is $\widehat{T}_{7,1}(\eta_7 = 3.6$#/100km-yr, $w_{7,1} = 263$cm, $R_{7,1} = 20\Omega) = 1.3858$. We can provide another example. For the Monte Carlo case ($h = 3$), the simulated BFR result $T_{7,3}(\eta_7 = 3.6$#/100km-yr, $w_{7_3} = 263$ cm, $R_{7,3} = 20\Omega)$ yields 1.2313 flashovers/100km-yr shown in Table 6, and the estimated one using the parameterized function (Eq. 19) is $\widehat{T}_{7,3}(\eta_7 = 3.6$#/100km-yr, $w_{7,3} = 263$cm, $R_{7,3} = 20\Omega) = 1.2374$. Figure 5 depicts the BFR parameterized function (Eq. 19) for the MC-EMTP procedure. Regression fitting factors $\alpha_{ij,h} \in \boldsymbol{\alpha_h}$ for all methods are listed in Table V. In all regressions, the Pearson coefficient is almost equal to 1. The resulting parameterized BFR functions are of high quality.

4.3 Optimization problem setup

Once determined the set of fitting parameters $\boldsymbol{\alpha_h}$ for each method h, the specific optimization formulation for each BFR procedure $h = \{1, 2, 3\}$ is written according to Eqs. 15–18 as:

$$\min_{\mathbf{w_h},\mathbf{R_h}} \sum_{k=1}^{12} N_k\sigma(w_{k,h} - w^b) + \sum_{k=1}^{12} N_k\beta\left[\frac{\rho_k}{R_{0k,h}}\right]^{\gamma} \tag{20}$$

subject to:

$$\widehat{T}_h = \sum_{k=1}^{12} \widehat{T}_{k,h}\frac{L_k}{L_T} = T^*$$

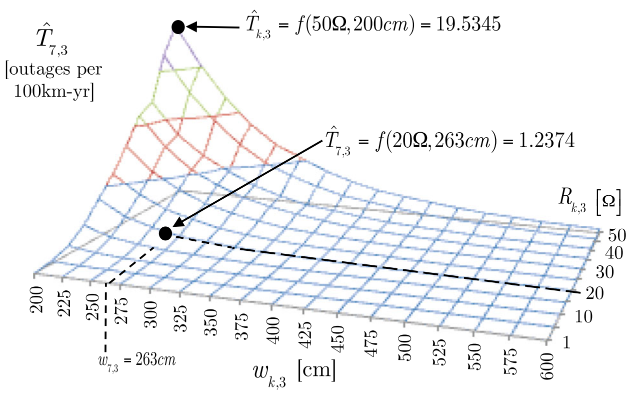

Fig. 5 Parameterized MC-EMTP BFR $\widehat{T}_{k,3}$

$$\widehat{T}_{k,h} = \sum_{i=1}^{6}\sum_{j=1}^{6} \alpha_{ij,h}\eta_k w_{k,h}^i R_{k,h}^j \; \forall k = 1, \ldots, 12$$

$$R_{0k,h} = \sqrt{\frac{\rho_k G_0 R_{k,h}}{\rho_k G_0 - 2\pi I_{ck,h} R_{k,h}^2}} \quad \forall k = 1, \ldots, 12$$

$$I_{ck,h} = 31 \sqrt[5/13]{\frac{\widehat{T}_{k,h}}{0.6\mu_k}} \quad \forall k = 1, \ldots, 12$$

$$200 \leq w_{k,h} \leq 445, 0 \leq R_{k,h} \leq 50 \quad \forall k = 1, \ldots, 12$$

where the earth ionization field gradient (G_0) is set equal to 500 kV/m, the length of the line is $L_T = 100$ km and line parameters by section, from $k = 1$ to $k = 12$ (N_k, w^b, ρ_k, η_k, L_k, H_k, b_k and w^{mx}) are provided in Table 5. The grounding cost model is characterized by $\beta = 55.52532416$ and $\gamma = 1.221891523$ as well as the insulation incremental cost (σ) is set in 15000 US\$/m [15]. The optimization models were solved with the Matlab's *fmincon* tool (interior-point method).

4.4 Optimization solution for a fixed $T^* = 1.4$#/100km-yr

The optimization problems were first formulated with a fixed rate of $T^* = 1.4$#/100km-yr. Each optimization problem has 24 state variables: 12 resistances $R_{k,h}$ and 12 insulation lengths $w_{k,h}$, $k = 1, \ldots, 12$, $h = 1, 2, 3$.

For the reference case $h = 1$ (EPRI), we are applying the method proposed in [15] with some differences. In [15], the parameterization of the BFR function was carried out with a polynomial order m=4 using a shadow length narrower than the used here. In this paper, we use a polynomial order m=6 and the shadow length suggested in [19]. However, the calculation of cumulative probabilities using the EPRI BFR evaluation method is the same in both cases.

The technical solutions by each case h and each section k: power frequency grounding resistances ($\boldsymbol{R_{0h}}$), impulse grounding resistances ($\boldsymbol{R_h}$), insulation lengths ($\boldsymbol{w_h}$) and resulting backflashover rates ($\boldsymbol{T_h}$) are depicted in Fig. 6a–d, respectively. The set of 12 power frequency grounding resistances $\boldsymbol{R_{0,h}}$ were obtained from Eq. 13. The set of resulting backflashover rates were obtained from Eq. 17.

The economic results (total costs and incremental costs) are listed in Table 8. Total costs correspond to the evaluation of objective function (Eq. 20) in million US\$. The incremental cost corresponds to the system λ_h (Lagrangian multiplier associated with Eq. 17).

The technical and economic results for the reference case (EPRI) shown in Fig. 6a–d and Table 8 coincide with the ones reported in [15].

Despite the EPRI, IEEE and MC-EMTP cases yielding different economic results, Fig. 6b shows the same resulting impulse grounding resistance for all cases. The reasoning that explain these differences in economic results is twofold. Firstly, each BFR parameterized function (Eq. 17) determines a different critical flashover current affecting the calculation of the power-frequency grounding resistances (Eq. 13) and therefore affecting the corresponding grounding costs (first row of Table 8). Secondly, each BFR function requires a different insulation scheme by section as seen in Fig. 6c affecting the insulation costs (second row of Table 8). As a result, Fig. 6d shows two patterns for the backflashover rate per section. The EPRI and IEEE cases have similar BFR pattern, and the MC-EMTP case shows wider variability. Figure 6a, c evidence lesser grounding and insulation reinforcement requirements in the MC-EMTP case in order to ensure an overall BFR of 1.4 flashovers/100km-yr. Notice how in all cases some backflashover rates are relaxed in sections k = 7-12 ($T_{k,h} > 1$) and some backflashover rates are adjusted below 1.4 in sections k=1-6 ($T_{k,h} < 1$).

In Table 8 we observe that IEEE and MC-EMTP cases yield the highest and lower total and incremental costs, respectively. The overall cost of the IEEE case is 25 % higher than the reference case (EPRI solution [15]). On the other hand, the MC-EMTP case is 11 % cheaper than the reference. Economic results are interpreted as follows. For example, for the IEEE case, the optimal solution requires a total investment of US\$ 3.37 million, US\$ 2.87 million in grounding electrodes and US\$ 0.44 million in insulation changes. The incremental cost of the BFR for the IEEE case is $\lambda_2 = \frac{\partial C_{G,2}}{\partial \hat{T}_{k,2}} = -2.02$ million US\$/flashovers/100km-yr. This means that a reduction of 0.01 flashovers per 100 km-yr requires an additional investment of US\$20200 in mitigation measures.

The EMTP model is showing more optimistic results from economic viewpoint. This means the EMTP method requires less investment in grounding and insulation to get the same reliability level produced by IEEE/EPRI methods. In other words, under the EMTP model we can allow higher resistances to achieve the same BFR obtained with IEEE/EPRI methods.

Table 7 BFR function fitting factors $\alpha_{ij,h} \in \boldsymbol{\alpha_h}$

	h = 1:EPRI[15]	h = 2:IEEE	h = 3:MC-EMTP
α_{11}	9.54548800E−01	2.15896621E−01	1.95823610E+00
α_{12}	1.30758684E−02	3.72286745E−01	−3.98106940E+00
α_{13}	4.61194491E−02	3.37945254E−02	9.09839552E−01
α_{14}	−2.57770923E−04	7.57089841E−04	−5.81992485E−02
α_{15}	−2.43460151E−05	−4.58081257E−05	1.76331919E−03
α_{16}	5.29926933E−07	5.07863954E−07	−2.57660471E−05
α_{17}	−3.55602222E−09	−1.10772662E−09	1.44019903E−07
α_{21}	−1.31319943E−02	−1.00090902E−03	−3.42121629E−02
α_{22}	1.27338972E−04	−5.45382098E−03	6.73202352E−02
α_{23}	−6.11546229E−04	−4.13684043E−04	−1.50300616E−02
α_{24}	2.88379414E−06	−8.87319227E−06	9.78536828E−04
α_{25}	4.06204012E−07	5.47222482E−07	−2.97215321E−05
α_{26}	−9.05450238E−09	−5.17138779E−09	4.31265051E−07
α_{27}	6.25041845E−11	6.53608217E−13	−2.37712802E−09
α_{31}	7.72680936E−05	−5.37785895E−07	−2.72206789E−05
α_{32}	−2.18882679E−06	3.20313170E−05	−3.41742441E−04
α_{33}	3.47423568E−06	2.41266879E−06	8.26666018E−05
α_{34}	−1.17807608E−08	2.89169569E−08	−5.37216794E−06
α_{35}	−2.79207038E−09	−2.24053684E−09	1.58547646E−07
α_{36}	6.29981252E−11	1.24534170E−11	−2.19890115E−09
α_{37}	−4.43118580E−13	1.21285403E−13	1.13668756E−11
α_{41}	−2.44250957E−07	8.63537415E−09	1.29453233E−06
α_{42}	1.05792821E−08	−9.62243201E−08	6.64756967E−07
α_{43}	−1.06038134E−08	−8.22964041E−09	−2.02728912E−07
α_{44}	1.75574675E−11	1.41113649E−11	1.28861589E−08
α_{45}	1.00884926E−11	2.96973849E−12	−3.50886540E−10
α_{46}	−2.28784990E−13	3.20484195E−14	4.26076458E−12
α_{57}	1.62997693E−15	−8.55339549E−16	−1.74753584E−14
α_{51}	4.33345916E−10	−9.29829715E−12	−4.83563680E−09
α_{52}	−2.39766484E−11	1.55632089E−10	−2.19347658E−10
α_{53}	1.81532919E−11	1.65278951E−11	2.16719051E−10
α_{54}	8.44643947E−15	−2.49335766E−13	−1.27277603E−11
α_{55}	−2.01573169E−14	3.11362614E−15	2.56123544E−13
α_{56}	4.57380527E−16	−1.98303078E−16	−1.13923109E−15
α_{57}	−3.28729975E−18	2.42727269E−18	−1.21027098E−17
α_{61}	−4.07091988E−13	−9.63850999E−15	6.98852919E−12
α_{62}	2.64215122E−14	−1.28104108E−13	−7.63705583E−13
α_{63}	−1.64422277E−14	−1.78861939E−14	−5.48971590E−14
α_{64}	−4.84266793E−17	4.65454710E−16	1.29178764E−15
α_{65}	2.10769591E−17	−1.13267378E−17	1.44584930E−16
α_{66}	−4.77197624E−19	3.25507399E−19	−5.64409501E−18
α_{67}	3.45025996E−21	−3.16069442E−21	5.61575484E−20
α_{71}	1.57783101E−16	1.43563197E−17	−3.59971036E−15
α_{72}	−1.14354208E−17	4.16742043E−17	6.60785756E−16

Table 7 continued

	h = 1:EPRI[15]	h = 2:IEEE	h = 3:MC-EMTP
α_{73}	6.13963440E−18	7.98282294E−18	−3.59805671E−17
α_{74}	3.53409740E−20	−2.73848553E−19	3.65689024E−18
α_{75}	−9.00185432E−21	7.71630334E−21	−2.06819061E−19
α_{76}	2.03039613E−22	−1.80573522E−22	4.81746241E−21
α_{77}	−1.47394090E−24	1.56517268E−24	−3.92900292E−23
R^2	0.99929876	0.99921987	0.99931787

Table 8 Summary of results for $T^* = 1.4$

Investment cost	BFR calculation method		
	h=1-EPRI[15]	h=2-IEEE	h=3-Monte Carlo
Grounding cost: C_{Gh} (M$)	2.41	2.87	2.28
Insulation cost: C_{Ih} (M$)	0.25	0.44	0.09
Total cost: C_{Th} (M$)	2.67	3.32	2.37
$\lambda_h = \frac{\partial C_{G,h}}{\partial T_{k,h}}$ (M$/#/100km-y)	−1.90	−2.02	−1.02

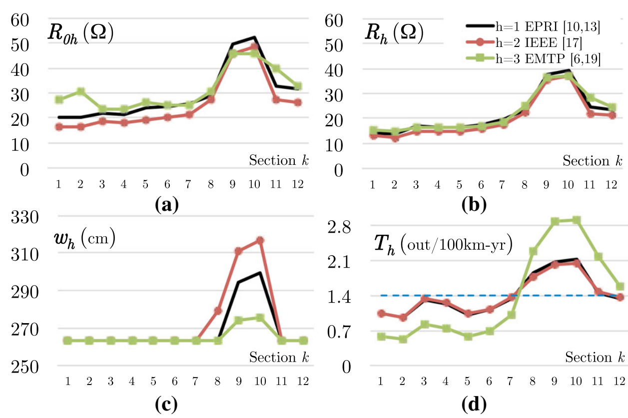

Fig. 6 Solution set by section for T^*=1.4: $\boldsymbol{R_{0h}}$, $\boldsymbol{R_h}$, $\boldsymbol{w_h}$ and $\boldsymbol{T_h}$

In Fig. 6d, the curve of the BFR associated with the EMTP model seems inverted with respect to IEEE/EPRI output since the optimization using the EMTP method shows a better ability to reduce the grounding cost in the first 8 sections than other two methods guaranteeing the same overall BFR level. This allows to relax the solution by specifying higher resistances in sections 9-12 in order to accomplish the desired reliability goal (T^*=1.4 #/100km-yr). The EMTP approach do not require lower resistances to achieve the goal. This outcome could be related to the front wave times used in the EMTP approach specified in [21,22] and listed in Table 3. However, more conservative front wave times can be used instead of. For a real project, it would be interesting to analyze how tower grounding and insulation economics are affected when different wave front times are considered.

4.5 Optimization solution for a range of T^* from 0.1 to 1.7

The optimization problems were formulated with BFR targets ranging from T^*=0.1 to T^*=1.7 in steps of 0.1 flashovers/100km-yr. A total $3 \times 17 = 51$ optimization problems with size $24 \times 51 = 1224$ state variables were defined and solved. Due to the lack of space, only economic solutions are provided, and technical solutions are not included, but they can be requested to the authors. Results of total and incremental curves are depicted in Fig. 7.

From Fig. 7a, we observe that the optimization method with IEEE and EPRI approaches yield the same incremental function (both curves, red and black are overlapped). The MC-EMTP approach showed lower marginal costs than the EPRI and IEEE cases. Notice from Fig. 7b that achieving performance rates higher than 0.5 flashovers/100km-yr will imply extraordinary expenditure efforts in all cases. In the range of 0.5–1.7 flashovers/100km-yr, the incremental curves remain stable as expected (Fig. 1). Results also show how IEEE/EPRI and MC-EMTP cases yield the highest and lowest total and incremental cost curves, respectively. The EPRI method shows intermediate total costs coinciding with the results reported in [15]. Incremental costs are obtained from Lagrange multipliers of the two variable nonlinear optimization model. As the problem is continuous, the first-order and second-order optimality conditions are obtained, necessary and sufficient conditions to guarantee a local minimum.

The differences in the optimal solution costs due to the distinct simulation models reflect how some models are more optimistic than others in the occurrence of the backflashover phenomenon. In this case, the MC-EMTP method yields optimistic results. As referred above, we used wave front times

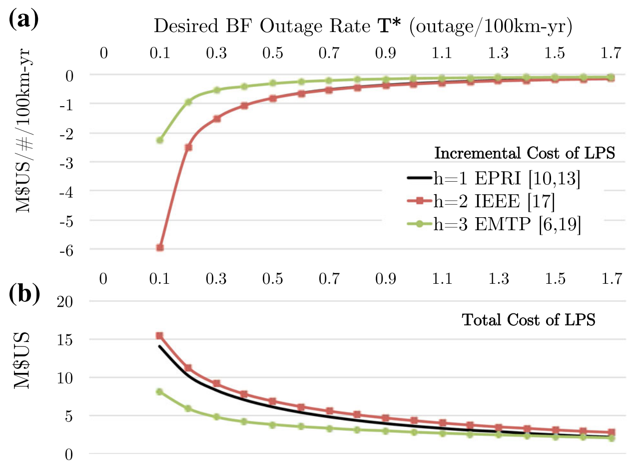

Fig. 7 Incremental and total cost of the S for T^*=[0.1-1.7]

(Table 3 [21,22]) larger than the ones used in the IEEE/EPRI approach. In order to evaluate the robustness of the optimization method under the MC-EMTP approach, we suggest to perform a sensitivity analysis considering more conservative wave front times, since currents with faster wave fronts are more likely to produce backflashover.

Getting a solution of the optimization problem using an evolutionary approach such as the Ant Colony System [27] would be useful to validate the results.

5 Conclusions

The IEEE Std. 1243-1997 and the Monte Carlo EMTP backflashover rate (BFR) evaluation procedures have been used to apply the modified Hileman's approach to optimize the costs of mitigation measures (grounding and insulation) with respect to the BFR evaluation methods. Solutions were compared with the results obtained by optimization model based upon the EPRI's two-point method.

We conclude that optimization formulations based on IEEE/EPRI and Monte Carlo-EMTP approaches yield the highest and lowest total and incremental cost curves, respectively, reflecting that the MC-EMTP method is the most optimistic calculation approach in the context of optimization tasks to ensure minimal cost of mitigation measures for a prescribed backflashover rate.

We highlight that all procedures (EPRI, IEEE and MC-EMTP) yield a similar pattern of impulse grounding resistances to assure a prescribed reliability level at minimum investment cost. The main aspect that justifies differences on overall costs lies on the determination of power-frequency grounding resistances as a function of impulse resistances.

Further research should be carried out to evaluate how the optimization results change when different impulse grounding resistances, front wave times and line arrester models are applied in the context of stochastic-based procedures to determine the BFR of transmission lines.

References

1. Chisholm Anderson JG (2005) EPRI AC transmission line reference book-200 kV and above, chapter 6, 3rd edn. Electric Power Research Institute, Palo Alto
2. Rudnick H, Palma R, Fernandez JE (1995) Marginal pricing and supplement cost allocation in transmission open access. IEEE Trans Power Syst 10(2):1125–1132
3. He J, Gao Y, Zeng R, Zou J, Liang X, Zhang B, Chang S (2005) Effective length of counterpoise wire under lightning current. IEEE Trans Power Deliv 20(2):1585–1591
4. Grosser GE, Hileman AR (1967) Economic optimization of transmission tower grounding and insulation. IEEE Trans Power Apparatus Syst 86(8):979–986
5. American Institute of Electrical Engineers (1950) A method of estimating lightning performance of transmission lines. Trans AIEE 69(2):1187–1196
6. Dommel HW (1986) Electromagnetic transients program (EMTP) theory book. Bonneville Power Administration, Portland
7. De Oliveira-De Jesus PM, Khodr H, Urdaneta AJ (2002) Model for optimum design of grounding electrodes of transmission line towers (Modelo para el diseño óptimo de electrodos de puesta a tierra en torres de transmisión, in Spanish), Proc. III Venezuelan Congress Electrical Engineering CVIE, November 26–29. Faculty Engineering Central University of Venezuela, Caracas, Venezuela 1:11–15. https://www.researchgate.net/publication/343917258
8. Electric Power Research Institute EPRI (1975) Transmission line reference book, 345 kV and above, 1st edn. Electric Power Research Institute, Palo Alto, CA
9. Ekonomou L, Iracleous DP, Gonos IF, Stathopulos IA (2006) An optimal design method for improving the lightning performance of overhead high voltage transmission lines. Electr Power Syst Res 76:493–499
10. Christodoulou CA, Ekonomou L, Harkiolakis N, Stathopulos IA (2009) Optimization of Hellenic overhead high-voltage transmission lines lightning protection. Energy 34(4):502–509
11. De Oliveira-De Jesus PM, Hernandez-Torres D, Urdaneta AJ (2018) Cost-effective optimization model for transmission line outage rate control due to backflashover phenomena. Electr Power Compon Syst 46(16–17):1834–1843
12. Electric Power Research Institute EPRI (1982) Transmission line reference book, 345 kV and above, 2nd edn. Electric Power Research Institute, Palo Alto, CA
13. Vega-Hincapie JD, (2017) Methodology for optimizing the level of electrical insulation and resistance to grounding in transmission lines in relation to their performance against atmospheric electrical discharges (in Spanish), M.Sc. Thesis dissertation, National University of Colombia. https://repositorio.unal.edu.co/handle/unal/62103
14. De Oliveira-De Jesus PM, Hernandez-Torres D, Urdaneta AJ (2018) Multiple objective approach for reliability improvement of electrical energy transmission systems exposed to backflashover phenomena. Electr Eng 100(4):2743–2753
15. De Oliveira-De Jesus PM (2019) A new method to determine incremental costs of transmission lightning protection systems. Electr Power Compon Syst 47(19–20):1759–1774
16. Hileman AR (1999) Insulation coordination for power systems. CRC Press, Boca Raton
17. Amaya JC and De Oliveira-De Jesus PM (2019) Economic optimization of the backflashover outage rate in HVDC transmission

systems. In: 2019 FISE-IEEE/CIGRE conference, December 3–6, Medellin, Colombia 1–6
18. Silveira FH, Visacro S, Souza RE (2017) Lightning performance of transmission lines: assessing the quality of traditional methodologies to determine backflashover rate of transmission lines taking as reference results provided by an advanced approach. Electric Power Syst Res 153:60–65
19. IEEE Std. 1243 (1997) IEEE guide for improving the lightning performance of transmission lines, New York: Institute of Electrical and Electronics Engineers, NY
20. CIGRE Working Group 01 of SC 33, (1991) Guide to Procedures for Estimating the Lightning Performance of Transmission Lines, Brochure No. 63, Paris, France
21. Sarajcev P (2015) Monte Carlo method for estimating backflashover rates on high voltage transmission lines. Electr Power Syst Res 119:247–257
22. Gatta FM, Geri A, Lauria S, Maccioni M, Santarpia A (2014) An ATP-EMTP Monte Carlo procedure for backflashover rate evaluation: a comparison with the CIGRE method. Electr Power Syst Res 113:134–140
23. Koehler F, Swingler J (2018) Analysis of flashover mitigation measures to improve the lightning performance of transmission lines. In: 2018 53rd international universities power engineering conference (UPEC), pp. 1–6. Sept. Glasgow, UK, pp 4–7
24. Nucci, CA (2010) A survey on Cigré and IEEE procedures for the estimation of the lightning performance of overhead transmission and distribution lines. In: 2010 Asia-Pacific international symposium on electromagnetic compatibility, pp 1124–1133. April 12–16, Beijing, China
25. Sunde ED (1968) Earth conduction effects in transmission systems, 2nd edn. Dover Publications Inc, New York
26. IEEE Std. 81 (2012) IEEE Guide for Measuring Earth Resistivity Ground Impedance and Earth Surface Potentials of a Ground System, New York: Institute of Electrical and Electronics Engineers
27. Alvarado JM, Alvarado EV, Arevalo MA, Quituisaca, SP, Gomez JF, De Oliveira-De Jesus, PM (2009) Ant colony systems application for electric distribution network planning. In: 15th international conference on intelligent system applications to power systems, pp 1–6, 8–12 November, Curitiba, Brazil